ICES Journal of Marine Science, 2026, Vol. 83, Issue 7, fsag137
https://doi.org/10.1093/icesjms/fsag137
Original article

Otolith-derived growth variations in red mullet (*Mullus barbatus*) reveal spatial heterogeneity under present and future climate scenarios

Pierluigi Carbonara [1,2], Matteo Chiarini [1,*], Loredana Casciaro [1,2], Cosmidano Neglia[1,2], Lola Toomey [1], Michele Palmisano[2], Andrea Bellodi [3,4], Maria Cristina Follesa [4], Walter Zupa [1,2]

[1]Fondazione COISPA ETS, 70126 Bari, Italy
[2]COISPA Tecnologia & Ricerca, 70126 Bari, Italy
[3]Department of Integrated Marine Ecology, Calabria Marine Center, Stazione Zoologica Anton Dohrn (SZN), 87071 Amendolara, Italy
[4]Department of Life and Environmental Sciences, University of Cagliari, 09126 Cagliari, Italy
*Corresponding author. E-mail: chiarini@fondazionecoispa.org

Abstract

Understanding how environmental variability shapes growth in marine fish is essential for predicting population dynamics under climate change. This study investigates spatial differences in the growth of red mullet (*Mullus barbatus*) across three neighbouring regions of the South Adriatic (GSA 18) and North-Western Ionian (GSA 19) Seas (central Mediterranean). Otolith increments widths were analysed to quantify life growth, while environmental drivers were assessed using diverse oceanographic variables, including sea surface temperature, bottom temperature, oxygen concentration, salinity, and chlorophyll concentration. Generalized additive models were fitted to identify the environmental and spatial factors influencing growth under both contemporary and projected climate conditions. Growth exhibited pronounced spatial heterogeneity, with distinct localized hotspots in both the eastern and western portions of GSA 18, reflecting fine-scale hydrographic variability. Temperature emerged as the primary environmental driver, with optimal growth estimated around 18.5°C. Forecasts under representative concentration pathway climate scenarios revealed a non-linear response: a mid-century enhancement in growth followed by a decline by 2099, linked to warming beyond the thermal optimum. These results underscore the significance of local environmental conditions in shaping growth trajectories and highlight the potential vulnerability of red mullet populations to future climate change. Otolith chronologies, combined with spatially explicit modelling, offer an effective framework for detecting environmental impacts on growth. Accounting for spatial and climate-related variability in growth may enhance the accuracy of current assessment models and support the development of climate-ready fisheries management strategies in the Mediterranean.

Keywords phenotypic plasticity, otolith growth increments, spatial growth patterns, climate change projections, *Mullus barbatus*

Introduction

Marine organisms' life-history traits are shaped by both natural and human-induced pressures. These forcings can impact both reproductive parameters (e.g. spawning periodicity, size, and age at sexual maturation, fecundity, and overall reproductive potential), as well as growth-related traits such as population demographic structure and intrinsic growth rate capacity (Daufresne et al. 2009, Pepin 2015, Morrongiello et al. 2025, Lojo et al. 2022). When these pressures are particularly intense or act persistently over long timescales, they may impose strong selective regimes that favour certain genotypes, leading to evolutionary changes within populations (Hollins et al. 2018). Therefore, understanding of the factors that drive variation in maturation schedules and growth trajectories is critical for anticipating species adaptive responses to rapid environmental alterations such as climate change (Dalgleish et al. 2010), habitat degradation (Öckinger et al. 2010), and sustained harvesting (Hobday et al. 2011).

A key biological indicator at the individual and population levels is growth rate, which is determined by how an individual's size varies during ontogenesis. It is highly sensitive to an array of intrinsic factors (e.g. physiological constraints and genetic background) and extrinsic drivers, including environmental fluctuations and human activities (Enberg et al. 2012, Morrongiello and Thresher 2015, Carbonara et al. 2022). The broad diversity in adult body sizes observed among fish species, from millimetre-scale minnows to multi-metre sharks, reflects wide differences in species-specific growth strategies. However, growth variability may also occur at the intraspecific level, depending on environmental conditions, resource availability, and life-history trade-offs (Wang and Ellis 1998, Pilling et al. 2002). Because organisms have finite energy resources, they must balance investment in somatic growth

Received: 23 December 2025. **Revised:** 30 June 2026. **Accepted:** 1 July 2026

with other essential vital activities, like reproduction, foraging, movement, and somatic development. This balance depends not only on intrinsic physiological and genetic factors (Debes et al. 2014, Morrongiello and Thresher 2015, Grønkjær 2016), but also on external drivers such as temperature regimes, food supply, and anthropogenic pressures like fishing intensity and/or pollution (Matthias et al. 2018, Kraak et al. 2019, Taslima et al. 2022, Carbonara et al. 2022, Gokul et al. 2023). The observed growth trajectory of any individual thus emerges from the interplay between its genetically determined growth potential and the specific environmental conditions in a broad sense it experiences throughout life (Chung et al. 2019, Karametsidis et al. 2023).

These complex interactions explain why spatial differences in habitat characteristics, productivity regimes, or exploitation histories can lead to differences in growth patterns, even between geographically adjacent areas (Aranha et al. 2009, Daufresne et al. 2009, Carbonara et al. 2022). Functionally, growth is a cornerstone life-history trait that shapes ecological dynamics (Edeline 2007, Enberg et al. 2012) and helps determine how populations respond to environmental change. It influences critical fitness components, including survival and reproductive success (Sogard 1997, Barneche et al. 2018), and underpins key population-level processes, such as recruitment (Bergenius et al. 2002), maturation schedules (Uusi-Heikkilä et al. 2015), and ultimately stock biomass and productivity (Stawitz and Essington 2019). Accordingly, growth is a valuable proxy for exploring spatial and temporal variability in fish ecology and for assessing how habitat differences shape population functioning.

In marine ecosystems, fishing is a major human activity that, by removing individuals at different trophic levels, modifies the energy flow among populations (Essington et al. 2006). Such removals can affect the energetic landscape of populations, potentially modifying growth patterns and influencing other energetically demanding processes, such as reproduction (Heino and Godø 2002, Barot et al. 2004, Enberg et al. 2012). These effects may contribute to the substantial growth variability observed among exploited populations, even when these populations exhibit relatively low genetic differentiation or are geographically close (Matić-Skoko et al. 2018, Carbonara et al. 2022). Fishing-induced changes in density, resource competition, or size-selective mortality can reshape energy allocation strategies and growth trajectories (Morrongiello et al. 2019). For example, size-selective harvesting can promote earlier maturation and faster juvenile growth (Uusi-Heikkilä et al. 2015), while increased metabolic demands associated with warming may restrict somatic growth due to limited energy availability (Neuheimer et al. 2011).

Obtaining robust growth data from marine fish populations is challenging. Field sampling is often costly, time-consuming, and susceptible to methodological inconsistencies. Growth estimates may differ depending on sampling approaches (fishery-dependent vs fishery-independent surveys), otolith or other hard structure preparation and interpretation methods, age-reading criteria, and the experience of technical staff (Kimura and Lyons 1991, Coggins et al. 2013, Smith et al. 2016, Hüssy et al. 2016, Carbonara et al. 2019). Consequently, these methodological sources of variability can become embedded within growth chronologies and complicate interpretations of long-term growth patterns (Stawitz et al. 2015). These issues may be resolved with the help of dendrochronological techniques applied to otolith increment data, which offer a way to reconstruct historical growth responses to environmental variability with reduced methodological bias (Weisberg 1993, Strom et al. 2004, Black et al. 2005).

Sustainable fisheries management depends on an accurate understanding of how fish populations respond to harvesting and environmental variability, including directional changes, such as ocean warming (Kjesbu et al. 2014, Audzijonyte et al. 2016, Le Bris et al. 2018). Traditionally, the impacts of harvest and environmental fluctuations were viewed independently: fishing was associated with reductions in population mean lengths, whereas climate variability was linked to changes in variance (Planque et al. 2010). However, recent work has highlighted the importance of their combined effects (Fatima et al. 2023). Higher adult mortality due to fishing can weaken recruitment and increase its sensitivity to environmental fluctuations (Rouyer et al. 2012, Bitetto et al. 2025). Harvest can alter reproductive timing, potentially disrupting synchrony between spawning and favourable environmental windows (Rogers and Dougherty 2018), and modify the expression of temperature-dependent growth through density- or behaviour-mediated mechanisms (Morrongiello et al. 2019). Habitat degradation caused by fishing can reduce carrying capacity, thereby heightening population vulnerability to additional environmental pressures (Brown et al. 2018). In contrast, fishing-induced reductions in density may, in some cases, facilitate better survival under suboptimal warming conditions (Ciannelli et al. 2004). Importantly, both harvesting (Schindler et al. 2010) and ocean warming (Morrongiello and Thresher 2015) have been shown to synchronize population dynamics across space. Elevated synchrony under fisheries or environmental stress reduces the potential for demographic rescue among populations (Heino et al. 1997) and can increase the likelihood of large-scale fishery collapse (Lobón-Cerviá 2009), whereas asynchronous dynamics (e.g. growth portfolios) can buffer climate-driven variability (Campana et al. 2023).

The red mullet (*Mullus barbatus* L., 1758) is a demersal species that inhabits sandy and muddy substrates along the continental shelf. It is widely distributed from the eastern Atlantic coasts of Europe and Africa to the Mediterranean and Black Seas. While it inhabits depths ranging from shallow coastal waters down to 300 m, it preferentially occupies areas between 20 and 200 m (Tserpes et al. 2002, 2019). Owing to its high commercial value, it is one of the most important species targeted by Mediterranean coastal fisheries. Notably, red mullet exhibits substantial plasticity in growth (Carbonara et al. 2018), suggesting that populations display fine-scale bioecological adaptations across their range. This makes the species a powerful model for evaluating spatial and temporal variability in growth and for understanding how environmental gradients shape life-history traits. Developing a clearer picture of these dynamics is essential for predicting population responses to ongoing anthropogenic change and for ensuring sustainable resource management (Schindler et al. 2010, Rouyer et al. 2012, Engen et al. 2018), Morrongiello et al. 2019). Moreover, despite the many uncertainties related to growth/age analysis of the red mullet (Carbonara et al. 2019), it is one of the few species for which otolith analysis has been validated for age determination (Carbonara et al. 2018).

In the present study, we analysed otoliths of *M. barbatus* collected from three regions of the South Adriatic and Ionian Seas (central Mediterranean) to investigate spatial differences in growth patterns. We incorporated a range of environmental predictors, such as sea surface temperature (SST), bottom temperature, oxygen concentration, salinity and chlorophyll as primary

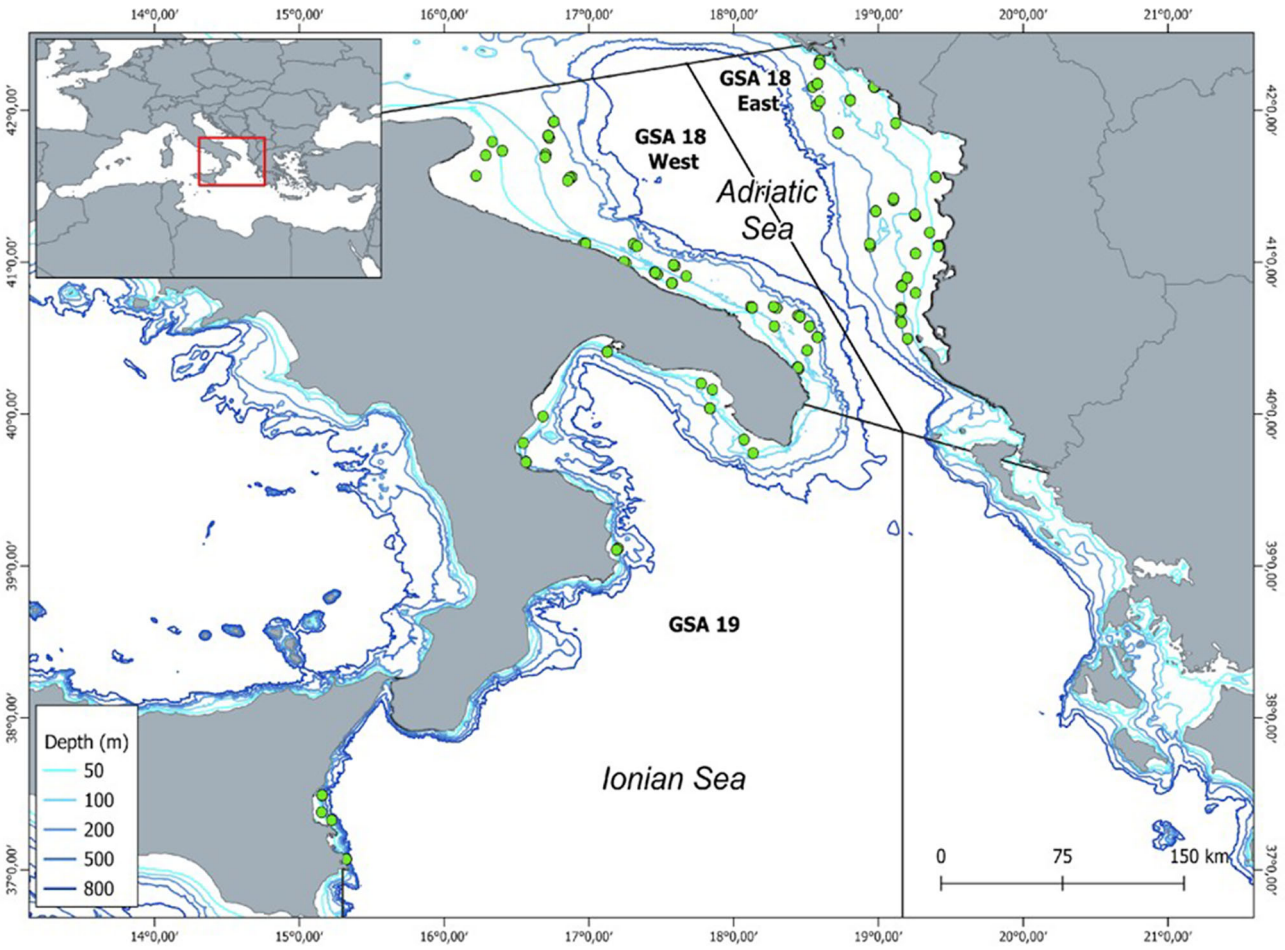

Figure 1 Visualization of the study areas: GSA 18WEST (west of the South Adriatic Sea), GSA 18EAST (east of the South Adriatic Sea), and GSA 19 (Western Ionian Sea). The points represent the hauls where the red mullets analysed in this work were captured.

production parameter, as well as yearly effects, in order to identify the environmental drivers of spatial growth variation. To further assess how growth patterns might shift under future climate conditions, we also evaluated projections under medium-term (2049) and long-term (2099) representative concentration pathway (RCP) scenarios. This combined ecological and climate-sensitive framework provides a basis for understanding how red mullet growth may respond to future environmental change.

Material and methods

Study fishery

The study area falls within two geographical sub-areas (GSAs *sensu* FAO-GFCM, https://www.fao.org/gfcm/data/maps/gsas/en/): South Adriatic Sea (GSA 18) and Western Ionian Sea (GSA 19). In order to investigate the spatial impact on the growth, otoliths were analysed from three areas: the west of the South Adriatic Sea (GSA 18WEST), the east of the South Adriatic Sea (GSA 18EAST), and the Western Ionian Sea (GSA 19) (Fig. 1).

The otoliths of red mullet specimens, caught during both fishery-dependent (monitoring of discard/landing of commercial species—Data Collection Framework EU Regulation 1004–2017) and fishery-independent (trawl survey MEDITS; Spedicato et al. 2019) monitoring within the three study areas, were used to take the measurements on the first growth increment.

Growth increment

The rings laid down on the otoliths are correlated along with the size of the red mullet specimens and, therefore, their growth (Carbonara et al. 2018, Carbonara and Follesa 2019). In general, fish species keep growing in size and weight, even after reaching sexual maturity (adult phase) (Charnov 2008, Alós et al. 2010), although the growth rate tends to decline as individuals get larger and older (Lester et al. 2004, Charnov 2008). In red mullet, sexual maturity is reached at the first year of life (Carbonara et al. 2015, 2018), so the growth rate is more pronounced within the first annual growth increment than in the older ones. In our analysis, In order to discriminate the effects of environmental parameters on the entire life cycle of red mullets, the first to fifth annual increments were taken into consideration. Otoliths were analysed whole, with the distal side up, under a stereomicroscope (Leica MC 170 HD) equipped with a microscope camera (Leica S9D). From each otolith, using the microscope camera software (Leica Application SuiteX), several measurements were taken in the posterior region along the longitudinal axis joining the sulcus and the nucleus (ICES., 2009), including otolith radius and winter rings' distance from the nucleus (R1, R2, …., Rn) (Fig. 2) was taken into

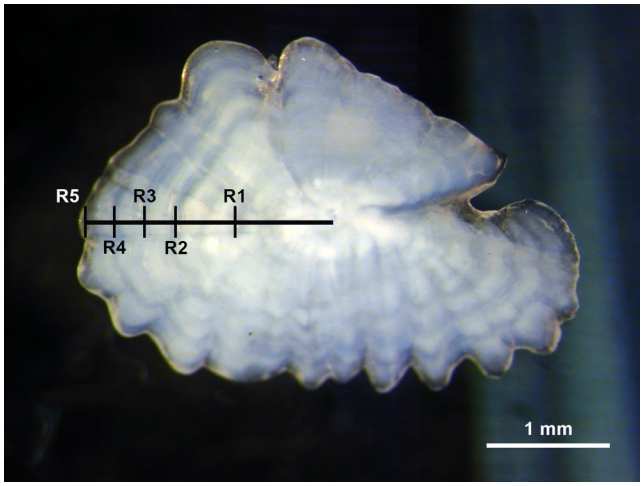

Figure 2 Growth pattern interpretation and definition of the measurement taken on Red mullet (*M. barbatus*) right otolith. R1, R2,…, R5 are the distance from the otolith' core of the first, second, …, third winter rings, respectively. As the catch year was 2014 (R5), the back-calculated deposition years for each annual increment are R4–2013, R3–2012, R2–2011, and R1–2010.

consideration for the spatial analysis. Moreover, based on age and year of capture, the year of deposition for each increment was back-calculated following methods proposed by Carbonara et al. (2018). The mean distance of the winter rings from the otoliths nucleus has been confronted within the three areas take into consideration (GSA 18WEST, GSA 18EAST, and GSA 19 through a Kruskall–Wallis test in R statistical environment (version 4.1.1; R Core Team 2026).

Environmental data

The spatial analyses were conducted testing the relative contribution of the following environmental variables: SST, bottom oxygen concentration (dox), bottom temperature (botTemp), bottom salinity (botso), and chlorophyl-a concentration (chl). The environmental data were obtained from 3D monthly Copernicus Climate Change Service data based on the POLCOM-ERSEM model (Copernicus 2020), which have a resolution of 1/10° (approximately 10 km). The monthly values of the environmental variables (SST, botTemp, botso, and chl) were averaged yearly, with the time series considered being 2004–2016. Climatic driver data underwent a bias-correction process, as described by Kuehn (2023), to correct the offset between historical environmental data and climate projections, allowing future projection of spatial distribution of otoliths growth along the study area.

Generalized additive model's analysis

Generalized additive models (GAMs) (Wood 2017) were applied to investigate and statistically test the impact of the environmental (SST, dox, botTemp, botso, and chl) and geographical (latitude, longitude) drivers on red mullet growth (otolith increments). GAM models were favoured over classical linear models and Generalized Linear Models because of their capacity to describe highly complex, nonlinear relationships when investigating both categorical and numeric explanatory variables. The data were modelled using the Gaussian error distribution, from the exponential family, with a log link function. Otolith increment distance was modelled using continuous fixed effects for environmental variables, including SST, dox, botTemp, so, botso, chl, alongside geographical, such as catch coordinates latitude (lat) and longitude (long). Conversely, the catch area (GSA 18WEST, GSA 18EAST, and GSA 19) and the incremental reference ring (year of deposition) were included in the model as random effects. Area was treated as a random effect to account for localized, site-specific variability in baseline growth rates that is not explicitly captured by the continuous environmental covariates, thus preventing spatial autocorrelation and unmeasured geographical bias. Similarly, the incremental reference ring was included as a random effect to account for the hierarchical structure of the data and inherent age-specific growth baseline variation. This allowed the model to control for the physiological deceleration of growth as individuals age (i.e. older rings are inherently narrower) and avoid pseudoreplication issues arising from multiple measurements associated with the same temporal/individual history. To reduce the risk of overfitting and promote parsimonious smooth selection, GAMs were fitted using the following settings: gamma = 1.4, which increases the effective degrees-of-freedom penalty during smoothness selection, and select = TRUE, which applies an additional shrinkage penalty allowing non-informative smooth terms to be penalized towards zero, following the model selection framework described by Wood (2017) and Marra and Wood (2011). Smoothing parameters were estimated using restricted maximum likelihood, REML, which provides stable and robust smoothness estimation for GAMs

The selection of meaningful variables to be included in the model was based on two complementary approaches. First, candidate predictors were screened for collinearity. Pairwise Pearson's correlation coefficients were computed, and variables showing a high degree of correlation ($|r| > 0.6$) were considered collinear. This screening was used as a preliminary diagnostic step rather than as an automatic exclusion rule. When correlated variables were identified, their inclusion was evaluated according to model performance, ecological relevance, and the interpretability of the fitted smooth terms. Second, a forward inclusion procedure was applied (Legendre and Legendre 1998, Wood 2001), in which covariates were added to the model sequentially. At each step, variables not already in the model were tested for inclusion, and retained only when they improved model fit, reduced Akaike information criterion (AIC), contributed to the deviance explained, and showed ecologically plausible effects. The assumptions underlying the application of GAMs were assessed graphically, and the corresponding diagnostics are reported in Figure S1.

Model fit was evaluated using the deviance explained, the AIC, the statistical significance of the smoothers associated to the explanatory variables ($P < .05$) and the ecological plausibility of the partial effects described by the spline functions. GAMs were fitted using the mgcv (Wood 2017) R package in R 4.5.2 (R Core Team 2026).

To assess whether temporal imbalance in sample size affected model inference, we performed a leave-one-year-out sensitivity analysis. The final model was refitted iteratively, each time excluding all observations from 1 year, and the resulting model performance was compared across iterations using deviance explained. This allowed us to evaluate whether the main results were disproportionately influenced by any single sampling year.

The selected model was used to produce future forecasts up to 2099. To estimate the overall growth pattern of the species, predictions were computed from the fixed-effect component of the model only, with the random effect of otolith ring deposition year set to zero. The resulting estimation therefore represented the average growth trajectory across deposition years. In particular, model projections have been based on the RCP taking into account the business-as-usual climate change scenario RCP 8.5 (Riahi et al. 2011). Climatic data, derived from the POLCOMS-ERSEM database produced using the marine ecosystem model, ERSEM v15.06 (European Regional Seas Ecosystem Model), coupled to the regional ocean circulation models, POLCOMS (the Proudman Oceanographic Laboratory Coastal Ocean Modelling System) (Copernicus Climate Change Service 2020), were bias corrected to reduce systematic deviations from observed conditions, ensuring consistency in mean, variability and distributional properties between modelled outputs and the reference observational dataset (Kuehn 2023).

The fitted model was finally used to extrapolate predictions for the following future years: 2029, 2039, 2049, 2059, 2069, 2079, 2089, and 2099.

The predicted spatial outcomes were reported as an index of relative change (RC) between the hindcast interpolation at 2016 and the extrapolated maps corresponding to the following periods: (i) mid-term (2049) and (ii) long-term (2099).

To assess the degree of environmental extrapolation in future projections, the ranges of the two climatic predictors retained in the final model, SST and botTemp, were compared between the model training period and future projection years. Minimum and maximum values observed in the training dataset, 2004–2016, were calculated and used as the reference environmental range. The corresponding minimum and maximum values were then extracted from the RCP 8.5 prediction grid for 2049 and 2099. Relative exceedance of future maximum values beyond the observed maximum was also calculated to quantify the extent to which projected conditions exceeded the calibration range of the model. These comparisons are reported in Table S1. In 2049, the degree of potential extrapolation was limited, as the projected maximum values exceeded the maximum observed during the training period by no more than approximately 10%. In contrast, by 2099 the exceedance was larger, indicating a higher level of extrapolation beyond the calibration range of the model. Projections for 2099 were therefore interpreted more cautiously, as they represent model extrapolations under environmental conditions partly outside those observed during model fitting.

The RC was estimated as the ratio between the value estimated for Period 1 or Period 2 and the sum of that value and the corresponding estimate for the present situation:

$$\text{Period 1 or 2} / \left(\text{Period 1 or 2} + \text{Present situation}\right).$$

An RC value equal to 0.5 indicates no change in growth. RC values greater than 0.5 indicate a local increase in the future scenario compared to hindcast, while RC values lower than 0.5 indicate a decrease.

Mapping

Distribution maps for both hindcast and forecast periods were estimated by predicting the annual maps on the GAM models, using a regular grid with a resolution of $0.042^\circ \times 0.042^\circ$. Predictions accounted for environmental variables selected in the final model, geographical variables (lat and long), and area factor (GSA 18EAST, GSA 18WEST, and GSA 19).

Results

Sampling took place between 2004 and 2016 (13 years) with 918, 1154, and 2507 measurements taken in GSA 18EAST, GSA 18WEST, and GSA 19, respectively (Table S2).

The size of the annual growth increments on otoliths grouped into three areas (GSA 18WEST, GSA 18EAST, and GSA 19) showed significant differences. In particular, GSA 18EAST showed a significantly larger first growth increment compared to GSA 18WEST and GSA 19 (Fig. 3). Considering that the otolith size is closely correlated with red mullet's body size (Carbonara et al. 2018), these results suggest the presence of significant spatial differences in red mullet growth patterns.

GAM modelling

The preliminary data exploration analysis was carried out for the numerical covariates, in order to assess the degree of correlation among them (Figure S2).

The SST, botTemp, lat, long, and GSA were significantly correlated with otolith increments in the time series considered (2004–2016) (Figs 4 and S2). The annual growth increment increased in size at SSTs higher than 18°C), before decreasing with rising temperatures until approximately 19°C (Fig. 4). There was then a slight increase in size before a further decrease above approximately 20°C (Fig. 4). The bottom temperature shows a clear dome-shaped pattern, with a maximum at 16°C. The average growth increment also appeared to present higher values at higher latitude and lower longitude (Fig. 4), corresponding to the area located in proximity of the Gargano promontory, in the western side of GSA 18. The model showing the best fit ($R^2 = 0.868$; AIC $= -18501$) and the highest explained deviance (86.9%) (Table 1) is the following:

$$\begin{aligned}\text{ring\_distance} \sim\ & \text{s}\left(\text{annual\_ring, bs} =' \text{re}'\right) + \text{s}\left(\text{long, lat}\right) \\ & + \text{s}\left(\text{SST}\right) + s\left(\text{gsa, bs} =' \text{re}'\right) + \text{s}\left(\text{botTemp}\right)\end{aligned}$$

The leave-one-year-out sensitivity analysis indicated that model performance was highly stable across iterations: deviance explained $= 0.869 \pm 0.002$. Deviance explained remained consistently high across refitted models, with limited variability around the mean value. Overall, these results support the robustness of the final GAM structure and suggest that the main spatial and environmental effects were not strongly affected by uneven sampling among years.

The selected GAM model includes the following numerical covariates: SST, bottom temperature (botTemp), latitude/longitude (lat, long) as fixed effects, together with random effect including the geographic area and the annual deposition ring (Table 1 and Fig. 4). In the analysed areas (GSA 18EAST, GSA 18WEST, and GSA 19), the northern–western side of the South Adriatic Sea (GSA 18 WEST) and the northern part of the GSA 19 and in the central part of the Eastern Adriatic Sea showed a higher red mullet growth pattern (Fig. 5).

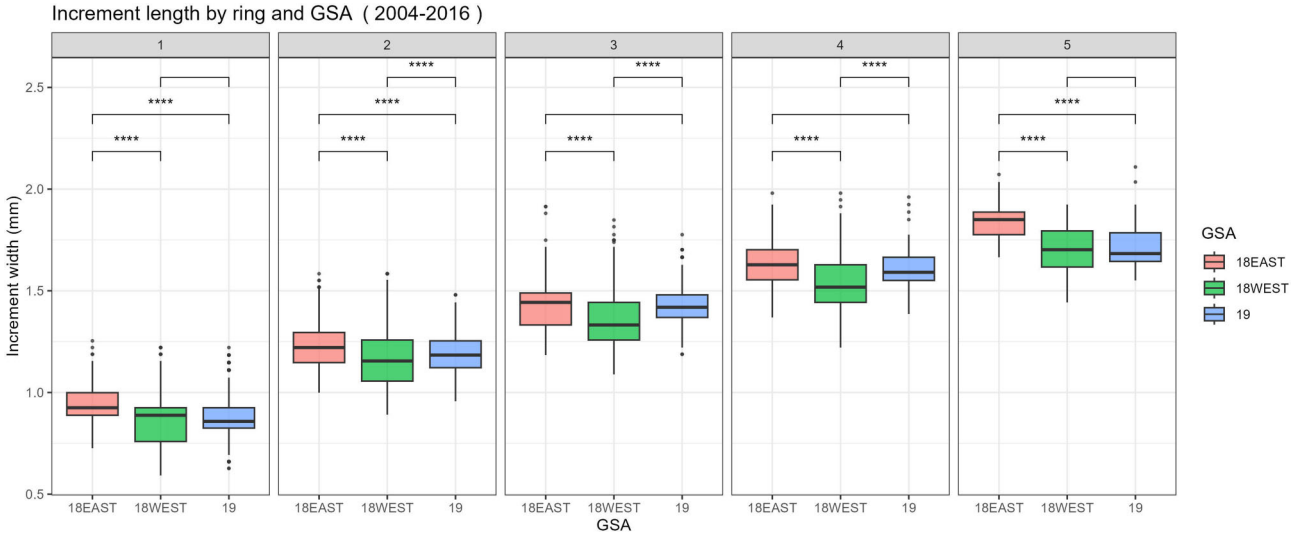

Figure 3 *M. barbatus* annual growth increments extension per area. The solid horizontal lines represent median values. The different lines over the boxplots represent the statistical pairwise comparison of the group areas conducted by Wilcoxon test (****$P \leq .0001$, significant level was set to 0.05).

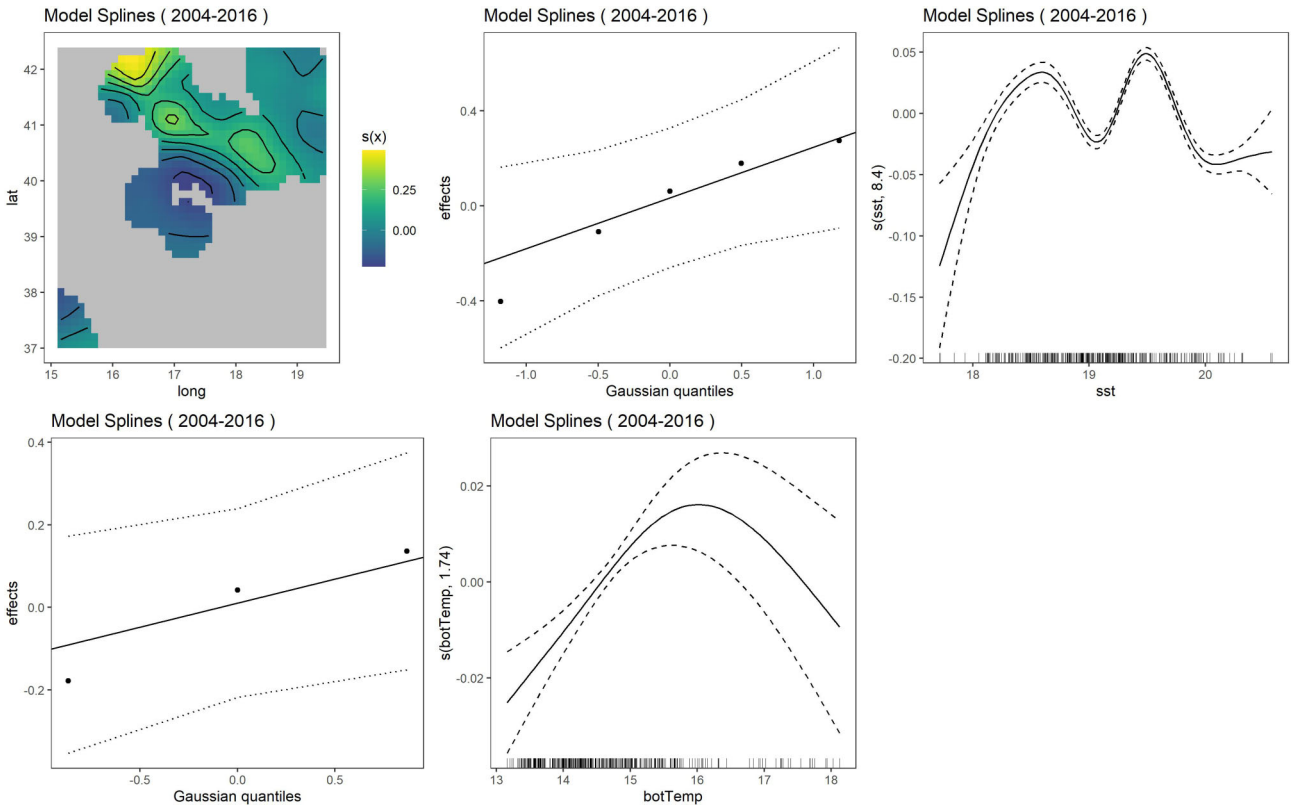

Figure 4 Effects of environmental and spatial predictors on the growth increment deposition in *M. barbatus*, estimated by a Gaussian GAM. From the top, following from the left to the right: spatial smooth of longitude and latitude (s(long, lat)); random effect on the annual ring of deposition; smooth effect of SST; random effect of the GSA effect; smooth effect of sea bottom temperature (botTemp). Solid line in smoothers represents the partial effects of the covariates included in the model, while dashed lines = ±2 SE; rug marks indicate data distribution. *Hindcast map.*

Forecast map

The forecast projection of the average annulus growth increment was calculated based on the climate change projection (RCP 8.5) and reported in the maps in Fig. S3 and in Fig. 6. In particular, Fig. 6 shows the distribution of predicted values across the three GSAs (18EAST, 18WEST, and 19) for the selected years 2016 (hindcast period), 2049, and 2099 (forecast period). GSA 18EAST generally shows a more compact distribution, with lower variability and fewer extreme values. GSA 18WEST shows greater dispersion, including several lower values, while GSA 19 presents a broader distribution and more pronounced upper-tail values, particularly in 2099.

Table 1. Main results of model selection according to the implementation of the forward inclusion of explicative variables.

Model formula	AIC	ΔAIC	Deviance explained	R^2
ring_distance ~ s(annual_ring, bs="re")	−16040		82.89	0.829
ring_distance ~ s(annual_ring, bs="re") + s(long,lat)	−17776	1736	85.80	0.858
ring_distance ~ s(annual_ring, bs="re") + s(long,lat) + s(SST)	−18448	672	86.79	0.867
ring_distance ~ s(annual_ring, bs="re") + s(long,lat) + s(SST) + s(gsa, bs="re")	−18470	21	86.81	0.868
ring_distance ~ s(annual_ring, bs="re") + s(long,lat) + s(SST) + s(gsa, bs="re") + s(botTemp)	**−18501**	**31**	**86.87**	**0.868**

Notes: For each model are reported the explained deviance in percentage, R^2, AIC, and the relative variation of AIC (ΔAIC) in comparison to the model in the previous step. The best model describing the correlation between the otolith increments (ring_distance) and environmental variables tested is highlighted in bold. All models used the Gaussian family distribution with the log link function

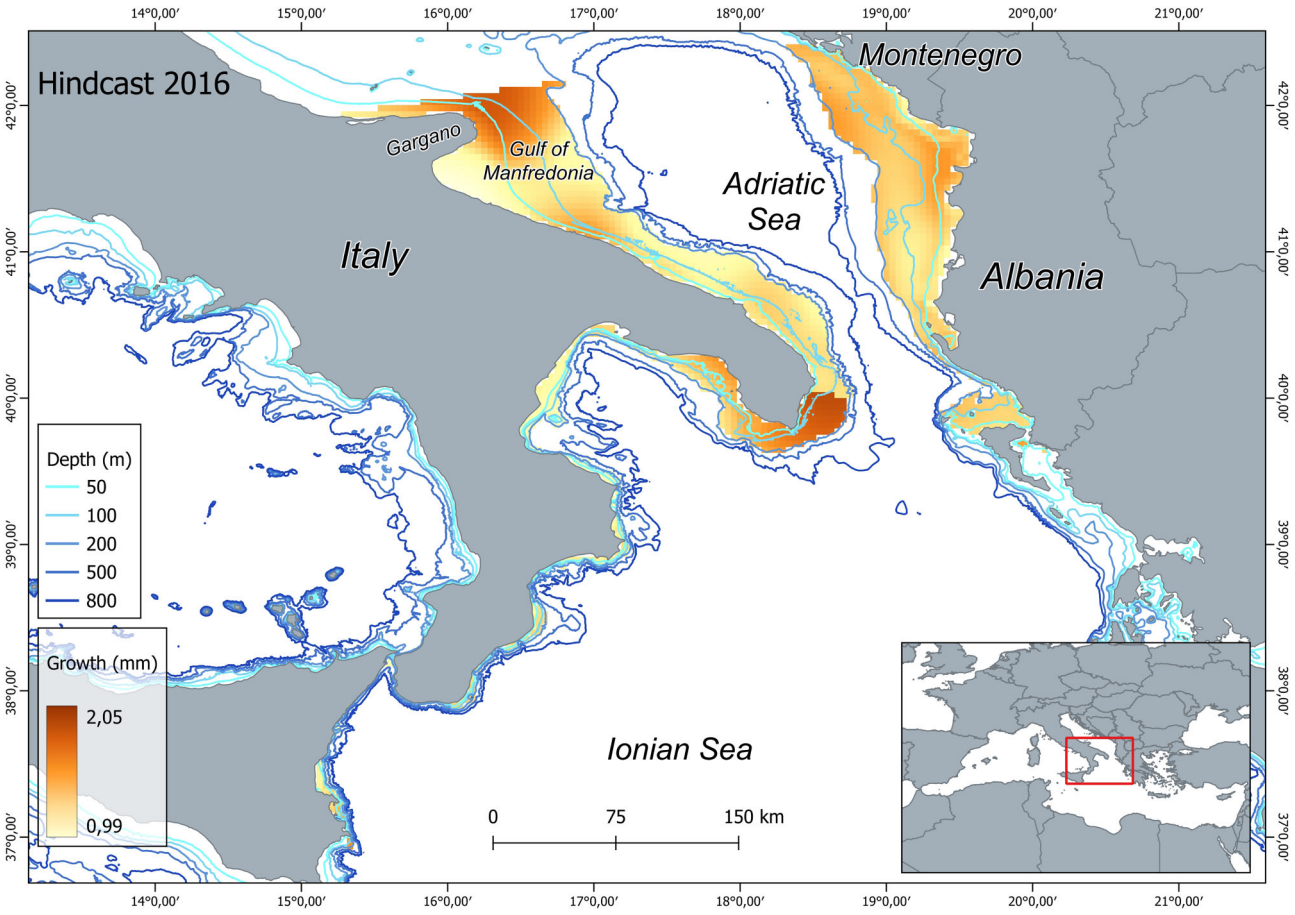

Figure 5 Spatial distribution of the GAM-predicted otolith growth of *M. barbatus* in the FAO GSAs 18 and 19. Colours represent the modelled mean annual growth increment.

In 2016, GSA 18EAST shows slightly higher median predicted values than the western side, while GSA 19 displays the widest range of values. In 2049, 18WEST has a slightly higher median than the other GSAs, although GSA 19 still shows substantial variability. By 2099, GSA 19 appears to have an increased occurrence of areas with relatively elevated predicted values.

Overall, a general increasing trend is observed up to the 2049 scenario, particularly in the GSA 18WEST (Fig. S3, panel d), in line with an increase in temperature foreseen by the RCP scenario. A global decrease in the growth pattern until 2099 was also suggested, in accordance with temperature splines (Fig. 4). Indeed, the RC analysis further supports this pattern. In the mid-term scenario (2049), the map shows higher occurrence of areas with values > 0.5 (Fig. 7), while in the long-term scenario (2099) a prevalence of RC values < 0.5 was reported, particularly in the more coastal areas (Fig. 8).

Discussion

A comprehensive analysis of growth variability in *M. barbatus* across three neighbouring regions of the Central-East Mediterranean basin (South Adriatic and North–Western Ionian Seas) was conducted providing new insights into the spatial and

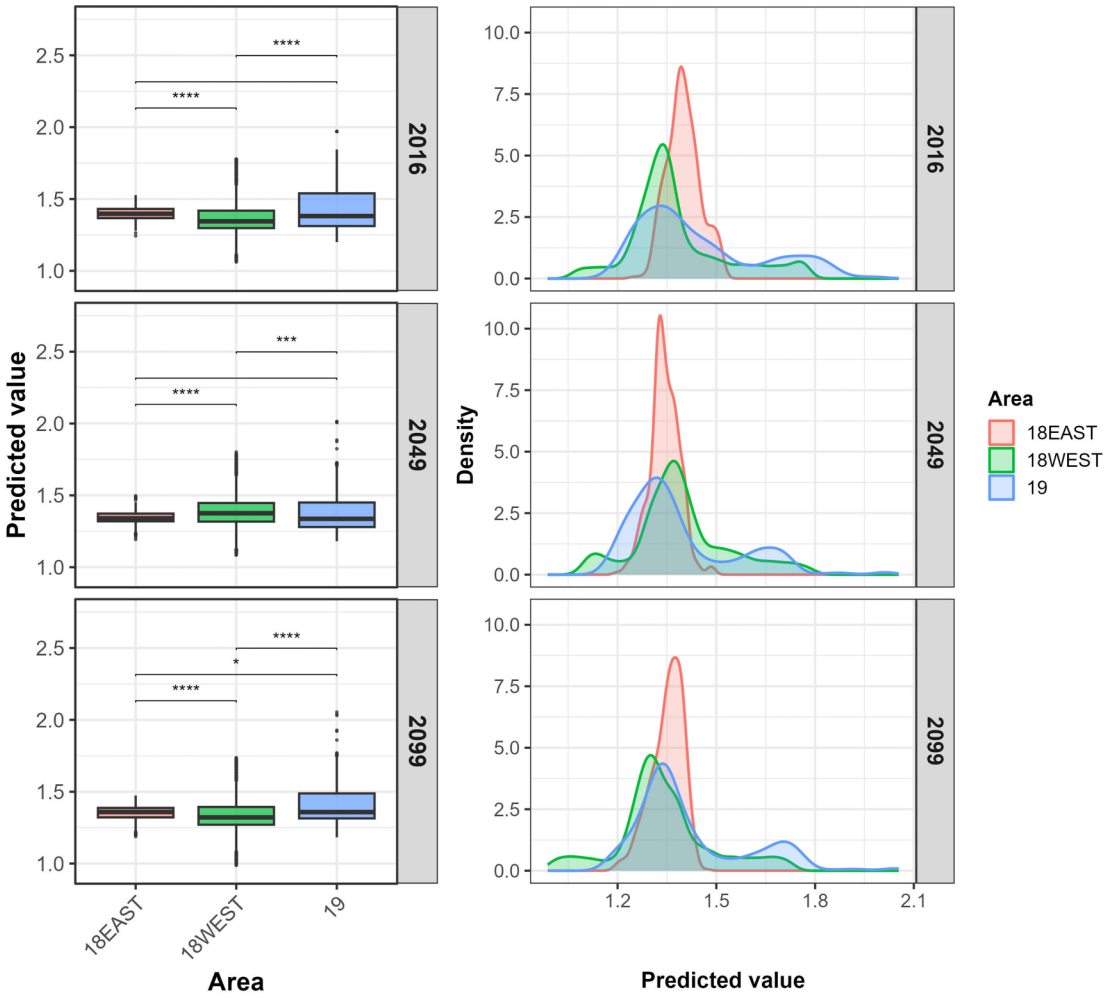

Figure 6 Distribution of predicted values across GSAs for the years 2016, 2049, and 2099. The left panels show boxplots summarizing the median, interquartile range, and variability of predicted values within each area, while the right panels show the corresponding Kernel density distributions. Pairwise differences among areas were tested using Wilcoxon rank-sum tests, with significant comparisons indicated by asterisks. The combined representation highlights both differences in central tendency and changes in the shape and spread of the predicted distributions among areas and periods.

environmental determinants of somatic growth for an ecologically and commercially important species. The integration of otolith increment measurements with environmental reconstructions and predictive modelling reveals strong spatial heterogeneity and sensitivity to temperature and habitat characteristics. These results support the assessment that red mullet present high phenotypic plasticity in growth, in accordance with previous findings for other Mediterranean demersal fishes that show substantial intra-specific variability also at small geographic scales (Pilling et al. 2002, Silva et al. 2008, Carbonara et al. 2022, Basilone et al. 2023). Growth in *M. barbatus* thus emerges as a dynamic life-history trait shaped by the interaction between intrinsic physiology, environmental drivers, and human pressures.

Spatial growth patterns

The comparison of otolith increment measurements across the three study areas revealed clear spatial heterogeneity in growth of *M. barbatus* within the South Adriatic–Ionian system. Rather than a simple east–west gradient, our results indicated a mosaic of localized growth hotspots distributed across both sides of GSA 18 (Fig. 5). Elevated growth occurred along the Montenegrin–Albanian coastal zone in GSA 18EAST, but also in the western Adriatic (Gargano Peninsula and the Gulf of Manfredonia) regions known for hydrographic retention (Ricci et al. 2024) and productive benthic communities (Cibic et al. 2022, Zupa et al. 2025). Such a spatial heterogeneity may reflect a portfolio-like structure in growth responses, enhancing population resilience to environmental fluctuations (Campana et al. 2023).

The spatial distribution of red mullet growth appears to be closely aligned with the hydrographic characteristics of the Adriatic Sea. The eastern part of GSA 18 is influenced by warmer and saltier Eastern Mediterranean waters, which are transported northwards along the Albanian and Montenegrin shelf (Vilibic and Orlic 2002). These water masses typically favour stratification, seasonal upwelling, and pulses of coastal productivity, enhancing the availability of benthic invertebrates, the red mullet's main prey (Vassilopoulou and Papaconstantinou 1993, Lambarte and Aguirre 1997, Chérif et al. 2011). Conversely, the western part of GSA 18 is affected by colder, fresher waters originating from the northern Adriatic Sea. While some western sectors are subject to riverine

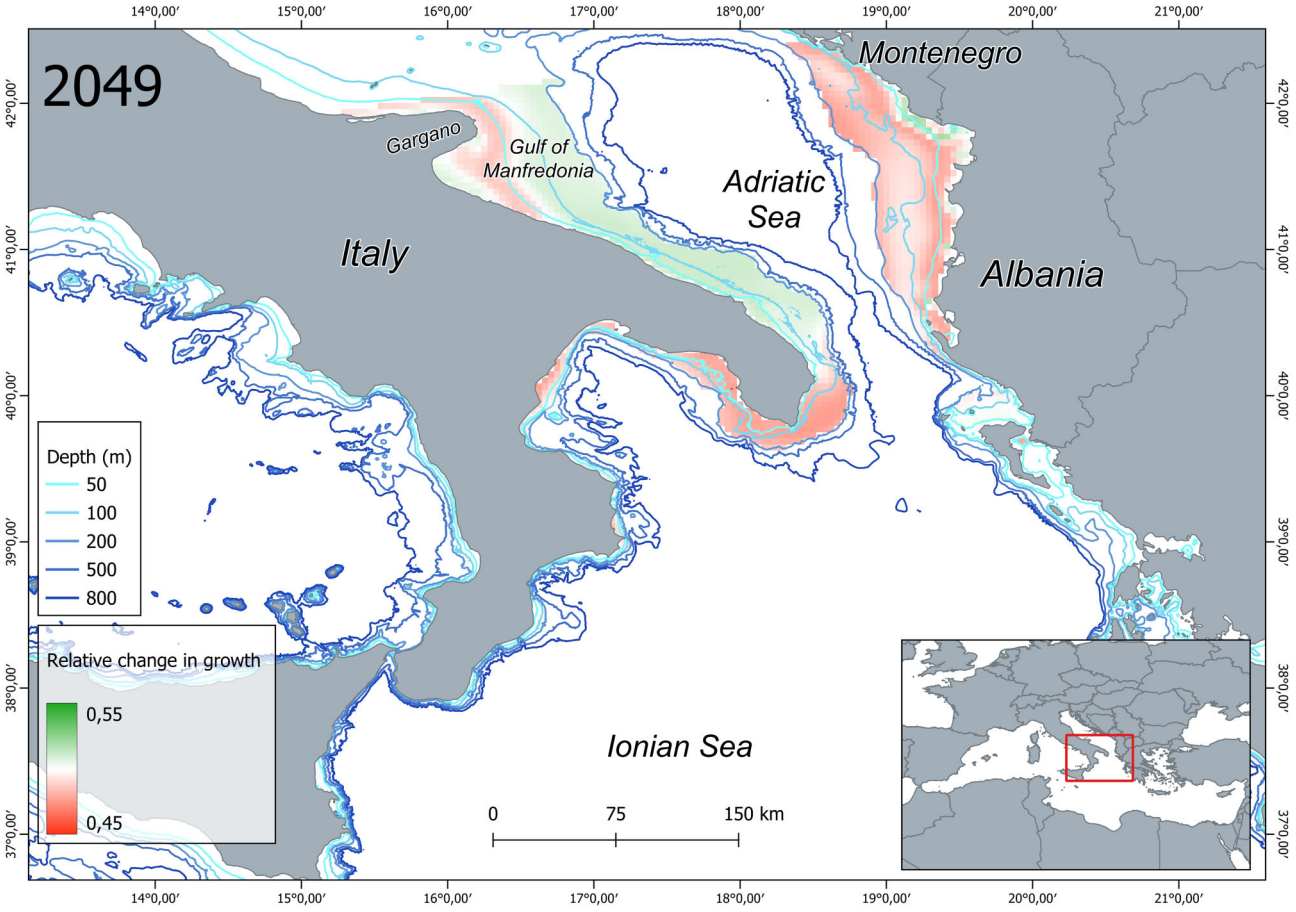

Figure 7 Spatial distribution of the RC in the GAM-predicted otolith growth of *M. barbatus* between the hindcast (2016) and the mid-term future climate scenario (2049) in the FAO GSAs 18 and 19. Colours represent the modelled RC in annual growth.

influence and turbidity events, the area around Gargano and the Manfredonia gyre benefit from hydrodynamic retention and recurrent nutrient recirculation (Lembo and Spedicato 2011, Rossi et al. 2024). This supports diverse and abundant benthic infauna. These processes might provide favourable feeding conditions for red mullet that could explain the presence of local high-growth zones.

The Ionian Sea (GSA 19) represents a different ecological domain, characterized by deeper basins, oligotrophic conditions, and high-salinity waters associated with Levantine Intermediate Water mass (Tursi et al. 2011). *M. barbatus*, which is constrained by energetic demands during the early stages of growth, may experience limited food availability compared to the more productive Adriatic shelf. This could explain the comparatively smaller increment widths observed in this area. However, in the north part of the GSA 19, where the shelf is wider and the cold water masses from the north interact with warm water masses originated from the south-eastern Mediterranean through the Otranto Channel (Tursi et al. 2011), red mullet growth appears to be higher. Interestingly, the spatial patterns identified by the GAM suggest that GSA 18WEST and GSA 19 may share more similar growth conditions than the two opposite Adriatic sectors (GSA 18EAST and GSA 18WEST), despite the latter being geographically closer. This apparent mismatch between geographic proximity and growth similarity likely reflects the complex hydrographic structure of the South Adriatic–Ionian system. The eastern Adriatic shelf is strongly influenced by the inflow of warmer and saltier Levantine waters, whereas the western Adriatic and northern Ionian sectors are more connected through circulation patterns, retention dynamics, and bottom-water characteristics. Consequently, local environmental conditions rather than simple geographic distance may play a stronger role in shaping growth variability in red mullet.

These spatial patterns support the hypothesis of a growth model in red mullet, which seems not only to be modulated at broad-scale by environmental gradients, but also by habitat characteristics at fine-scale (e.g. sediment type, benthic fauna composition, and hydrodynamic patterns) (Paradinas et al. 2020, Sinopoli et al. 2025). The observed differences align with evidence from other demersal species showing that local habitats may impose strong constraints on growth, notwithstanding a homogenous genetic structure (Rahikainen and Stephenson 2004, Aranha et al. 2009, Matthias et al. 2018). For red mullet, which is known to exhibit subtle genetic differentiation across the Mediterranean (Massa et al. 2025), these findings highlight the primacy of environmental heterogeneity, rather than genetic divergence (Massa et al. 2025), in explaining growth variability (Carbonara et al. 2018).

About environmental variables considered, the climate-related gradients (SST and botTemp) emerged as the strongest growth predictor. This is consistent with the literature demonstrating that temperature profoundly influences the metabolic rate, feeding behaviour, and energy allocation of ectotherms (Neuheimer et al. 2011, Enberg et al. 2012, Morrongiello et al. 2019). Growth in fish typically follows a unimodal thermal performance curve: it

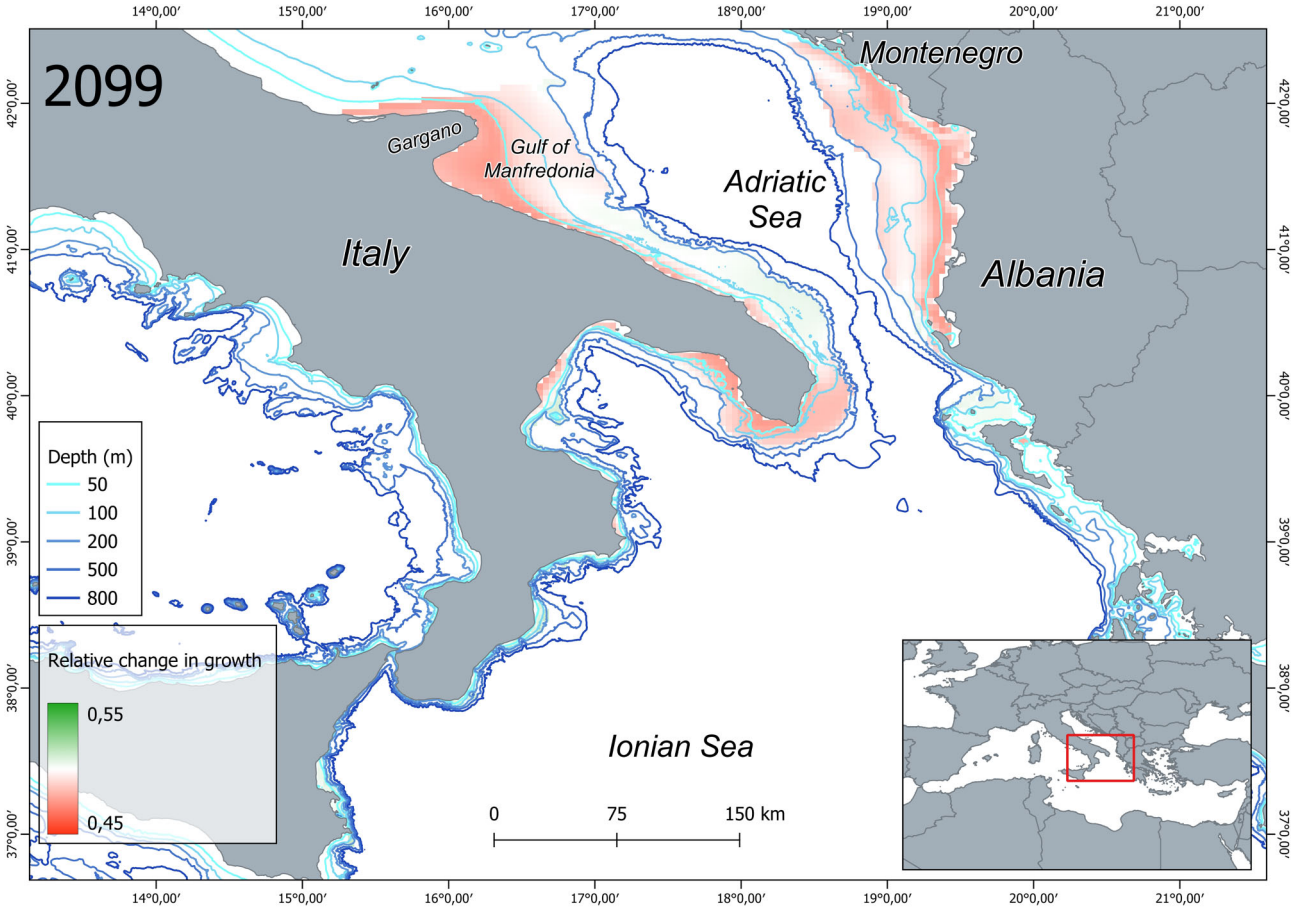

Figure 8 Spatial distribution of the RC in the GAM-predicted otolith growth of *M. barbatus* between the hindcast (2016) and the long-term future climate scenario (2099) in the FAO GSAs 18 and 19. Colours represent the modelled RC in annual growth.

increases with temperature up to an optimum, beyond which it declines as rising metabolic demands surpass the energy obtained from food (Daufresne et al. 2009, Neuheimer et al. 2011). The spline functions obtained from the GAMs clearly illustrate this relationship, indicating optimal growth at SST values between approximately 18.5 and 19.5°C and at bottom temperature (botTemp) of around 16.5°C. Below this threshold, increasing SST or bottom temperature likely enhances physiological functioning, digestion, and activity, thus promoting faster somatic growth. However, temperatures exceeding this threshold impose metabolic constraints, by increasing basal metabolic costs while reducing the energy available for growth (Heino and Kaitala 1996, Charnov 2008). This is consistent with studies showing that warming beyond optimal levels leads to reduced growth, smaller adult size, or shifts in size-at-age (Daufresne et al. 2009, Wakefield et al. 2016, Martino et al. 2019).

The dominance of temperature in the growth models does not imply that other variables are unimportant. Rather, it reflects the central metabolic role of thermal conditions and their ability to influence multiple physiological processes. Nevertheless, the inclusion of spatial smoothers (latitude/longitude) significantly improved model performance, indicating that temperature effects vary geographically and interact with local habitat features. Such modulation predicts that habitat productivity, prey availability, and hydrodynamic regimes outline how temperature influences growth patterns (Matthias et al. 2018, Morrongiello et al. 2019). This predominance of environmental control over demographic structure has also been reported in tropical systems, where growth variability appeared primarily shaped by environmental gradients rather than intrinsic population differences (Ng et al. 2025).

In the forecast (RCP 8.5), the increase in temperature also has consequences for other environmental factors, such as oxygen concentration, particularly towards the end of the projected century. This shift likely reflects the projected deoxygenation of Mediterranean bottom waters driven by warming, enhanced stratification and reduced ventilation (Reale et al. 2022). Deoxygenation has major implications for benthic fish, as reduced oxygen limits aerobic scope, thereby potentially restricting available energy for growth and forcing reallocation of energy towards maintenance processes (Audzijonyte et al. 2016).

The growing significance of bottom temperature in forecasts is also consistent with the predicted deepening of the thermocline and the warming of the bottom layers (Chimienti et al. 2021). As red mullet spends much of their juvenile and adult life near the seabed, bottom temperature directly influences its metabolism (Enberg et al. 2012). Therefore, the combined effects of warming and oxygen depletion in bottom waters can impose strong physiological constraints, which could outweigh any short-term benefits of warmer conditions (Audzijonyte et al. 2016).

This transition from surface-driven to bottom-driven environmental control suggests that red mullet may experience greater

physiological stress in the deeper or more stratified waters of the Ionian Sea and the southern Adriatic. The results also highlight that the relative importance of environmental variables may be further accentuated by climate change.

One of the most striking outcomes of our predictive modelling is the non-monotonic trajectory of future growth. Mid-century projections suggest significant growth enhancement, notably around 2049, followed by a general decline towards 2099. This pattern likely reflects the crossing of species-specific thermal thresholds, where initial warming may enhance metabolic performance, but further increases in temperature may lead to physiological stress and reduced growth efficiency.

The RC maps corroborate this interpretation: values above 0.5 dominate the mid-century scenario, while values below 0.5 dominate the late-century scenario. Such 'warming benefit windows' have been observed in several ectotherms, where transient improvements are followed by long-term declines (Neuheimer et al. 2011). In the case of red mullet, the mid-century productivity boost could temporarily increase biomass and recruitment (Maravelias et al. 2007, Tserpes et al. 2019), but this effect is unlikely to persist under RCP 8.5 conditions.

Despite our data referring to a relatively small spatial domain and for this reason, potential comparison with other areas or even species should be made with caution, the complex scenario observed highlights the importance of accounting for non-linear responses when evaluating climate impacts on marine populations. Apparent short-term benefits could mask longer-term declines, therefore emphasizing the need for adaptive and climate-informed management strategies.

Climate-driven growth changes and implications for assessment

Although fishing pressure was not analysed explicitly in this study, it is important to acknowledge that exploitation can also indirectly influence growth dynamics in *M. barbatus*. For instance, demersal trawling can alter benthic habitats and prey communities (Jennings et al. 2001, Ragnarsson and Lindegarth 2009, Mangano et al. 2017), which could potentially modify trophic conditions. Meanwhile, size-selective harvesting may lead to phenotypic or demographic shifts in growth patterns (Fiorentino et al. 2008, Kraak et al. 2019, Carbonara et al. 2022). Integrating fishing effort with environmental variables would help disentangle these effects in future studies. Beyond the potential impact of fishing, our results emphasize the value of otolith-based approaches in interpreting the influence of the environment on growth. Although otolith dendrochronology can be costly and time-consuming (Stawitz et al. 2015), it provides a fishery-independent source of data, as back-calculation allows observations at ages that are rarely sampled due to gear selectivity (López-Abellán et al. 2008, Ballagh et al. 2011). Moreover, otoliths preserve historical information on individual growth, enabling the reconstruction of growth trajectories that extend beyond the timeframe covered by contemporary size-at-age data (Begg et al. 2005). Therefore, conversely to length–age data, which can be affected by sampling biases and reader variability (Kimura and Lyons 1991, Coggins et al. 2013), otolith increments offer a high-resolution biological archive of the phenotypic responses of fish to environmental variability, food availability, and physiological processes. For *M. barbatus*, for which robust age criteria have been validated in the Southern Adriatic (Carbonara et al. 2018), increment-based analyses can be used to reconstruct growth histories even where length-at-age data are limited. Otolith-based growth indices have been widely used to detect climatic synchrony, density dependence, and long-term growth shifts in other species (Black et al. 2005, Stawitz et al. 2015, Martino et al. 2019), illustrating their broad usefulness in integrating climate and ecology. Recent applications of otolith chronologies have further demonstrated their ability to resolve distinct environmental sensitivities within and among populations, highlighting their power to link individual growth trajectories with environmental variability (Widdrington et al. 2025).

Moreover, otoliths remain a valuable resource for fisheries management, serving as inputs for stock assessment models (Reeves 2003, Carbonara et al. 2019) and as ecological indicators (Begg et al. 2005, Grønkjær 2016, Carbonara et al. 2022). In this regard, this study demonstrates that otolith chronologies, when coupled with flexible spatial GAMs, can effectively identify the growth environmental drivers and are well-suited to climate-change research, as they can accommodate non-linear responses, multi-variable interactions, and spatio-temporal complexity.

The strong spatial heterogeneity in growth observed here also has important implications for fisheries assessment and management. Stock assessment models often assume homogeneous growth within management areas such as GSAs, yet our results challenge this assumption. Spatial variability in growth affects estimates of size-at-age, natural mortality, spawning stock biomass, and recruitment potential (Thorson and Minte-Vera 2016). Therefore, maintaining uniform growth parameters across regions may lead to biased assessments and inappropriate harvest strategies. Therefore, adaptive models that incorporate environmental covariates or use climate-linked growth indices (Lee and Punt 2018) can help to anticipate shifts in productivity and reduce structural model uncertainty.

Although the projected mid-century growth enhancement suggests a temporary increase in potential yields, this period is expected to be short-lived. If management strategies respond to this transient improvement by increasing fishing pressure, this could accelerate long-term declines as warming intensifies. Conversely, protecting areas that currently support high growth, such as GSA 18EAST, could help buffer populations against late-century climate stress. Therefore, a nuanced understanding of the combined effects of environmental change and exploitation will be essential for designing resilient, climate-ready management strategies.

An important limitation of the present forecasting framework is the implicit assumption that current growth–environment relationships remain stationary through time. In reality, prolonged climate change may alter these relationships through physiological acclimation, evolutionary adaptation, shifts in prey composition, or broader ecosystem reorganization (Audzijonyte et al. 2016, Morrongiello et al. 2019). For example, changes in benthic prey communities, trophic interactions, or metabolic tolerance could modify the response of red mullet growth to warming and oxygen depletion over future decades (Neuheimer et al. 2011, Enberg et al. 2012). Consequently, the projected growth trajectories presented here should be interpreted as conditional scenarios based on the persistence of present-day ecological relationships, rather than deterministic predictions of future population dynamics.

Conclusions

This study demonstrates that growth in *M. barbatus* is a highly plastic, spatially structured, and environmentally sensitive life-history trait strongly influenced by temperature and local habitat conditions. Projected climate change may initially enhance growth but is likely to lead to declines as thermal and oxygen thresholds are exceeded. Incorporating spatial and environmental variability into assessment frameworks could be thus essential to improve predictions and support climate-ready fisheries management. Indeed, as climate change continues to reshape Mediterranean marine ecosystems, it will be crucial to develop adaptive, climate-informed strategies that account for spatial growth variability in order to ensure the long-term sustainability of red mullet and other demersal resources.

Acknowledgements

The authors are grateful to the anonymous reviewers for their constructive comments and suggestions, which greatly helped to improve the manuscript.

Author contributions

Pierluigi Carbonara (Conceptualization [equal], Formal Analysis [equal], Funding acquisition [equal], Investigation [equal], Methodology [equal], Resources [equal], Visualization [equal], Writing – original draft [equal], Writing – review & editing [equal]), Matteo Chiarini (Methodology [equal], Writing – original draft [equal], Writing – review & editing [equal]), Loredana Casciaro (Methodology [equal], Writing – review & editing [equal]), Cosmidano Neglia (Formal Analysis [equal], Methodology [equal], Visualization [equal], Writing – review & editing [equal]), Lola Toomey (Methodology [equal], Writing – original draft [equal], Writing – review & editing [equal]), Michele Palmisano (Methodology [equal], Writing – review & editing [equal]), Andrea Bellodi (Methodology [equal], Visualization [equal], Writing – original draft [equal], Writing – review & editing [equal]), Maria Cristina Follesa (Methodology [equal], Writing – review & editing [equal]), Walter Zupa (Formal Analysis [equal], Investigation [equal], Methodology [equal], Writing – original draft [equal], Writing – review & editing [equal]).

Supplementary material

Supplementary material is available at *ICES Journal of Marine Science* online.

Conflicts of interest

No declared.

Funding

This research has received funding from the European Union's Horizon 2020 Research and Innovation Programme under Grant Agreement number 101000318–shaping ecosystem based fisheries management (SEAwise). The data used in this study were collected according to the Data Collection Framework (DCF), which is supported by the Italian Ministry of Agriculture, Food Sovereignty and Forestry (MASAF) and the European Commission (EU Regulations 1004/2017).

Data Availability

The data underlying this article will be shared on reasonable request to the corresponding author.

References

Alós J, Palmer M, Balle S *et al.* Individual growth pattern and variability in *Serranus scriba*: a Bayesian analysis. *ICES J Mar Sci* 2010;**67**:502–12. https://doi.org/10.1093/icesjms/fsp265

Aranha A, Menezes G, Pinho MR. Biological aspects of the velvet belly, *Etmopterus spinax* (Linnaeus 1758) off the Azores, North East Atlantic. *Mar Biol Res* 2009;**5**:257–67. https://doi.org/10.1080/17451000802433175

Audzijonyte A, Fulton E, Haddon M *et al.* Trends and management implications of human-influenced life-history changes in marine ectotherms *Fish Fish* 2016;**17**:1005–1028. https://doi.org/10.1111/faf.12156

Ballagh AC, Welch D, Williams AJ *et al.* Integrating methods for determining length-at-age to improve growth estimates for two large scombrids. *Fish Bull* 2011;**109**:90–100.

Barneche DR, Robertson DR, White CR *et al.* Fish reproductive-energy output increases disproportionately with body size. *Science* 2018;**360**:642–5. https://doi.org/10.1126/science.aao6868

Barot S, Heino M, O'Brien L *et al.* Estimating reaction norms for age and size at maturation when age at first reproduction is unknown. *Evol Ecol Res* 2004;**6**:659–78.

Basilone G, Ferreri R, Aronica S *et al.* Growth variability in Atlantic horse mackerel *Trachurus trachurus* (Linneus, 1758) across the central Mediterranean Sea: contrasting latitudinal gradient and different ecosystems. *Front Mar Sci* 2023;**10**:1161552. https://doi.org/10.3389/fmars.2023.1161552

Begg GA, Campana SE, Fowler AJ *et al.* Otolith research and application: current directions in innovation and implementation. *Mar Freshw Res* 2005;**56**:477–83. https://doi.org/10.1071/MF05111

Bergenius MA, Meekan MG, Robertson RD *et al.* Larval growth predicts the recruitment success of a coral reef fish. *Oecologia* 2002;**131**:521–5. https://doi.org/10.1007/s00442-002-0918-4

Black BA, Boehlert GW, Yoklavich MM. Using tree-ring cross dating techniques to validate annual growth increments in long-lived fishes. *Can J Fish Aquat Sci* 2005;**62**:2277–84. https://doi.org/10.1139/f05-142

Brown CJ, Broadley A, Adame MF *et al.* The assessment of fishery status depends on fish habitats. *Fish Fish* 2018;**20**:1–14. https://doi.org/10.1111/faf.12318

Bitetto I, Martiradonna A, Zupa W *et al.* Climate change, stock productivity, and demersal fisheries management: a central Mediterranean case study. *Can J Fish Aquat Sci* 2025;**82**:1–15. https://doi.org/10.1139/cjfas-2024-0382

Campana SE, Smoliński S, Black BA *et al.* Growth portfolios buffer climate-linked environmental change in marine systems. *Ecology* 2023;**104**:e3918. https://doi.org/10.1002/ecy.3918

Carbonara P, Follesa MC (eds). *Handbook on Fish Age Determination: A Mediterranean Experience*. Rome: FAO. 2019, 192 pp.

Carbonara P, Ciccolella A, De Franco F *et al.* Does fish growth respond to fishing restrictions within marine protected areas? A case study of the striped red mullet in the South-West Adriatic Sea (Central Mediterranean). *Aquat Conserv: Mar Freshw Ecosyst* 2022;**32**:1–13. https://doi.org/10.1002/aqc.3776

Carbonara P, Intini S, Kolitari J *et al.* A holistic approach to the age validation of *Mullus barbatus* L., 1758 in the Southern Adriatic Sea (Central Mediterranean). *Sci Rep* 2018;**8**:1–19. https://doi.org/10.1038/s41598-018-30872-1

Carbonara P, Intini S, Modugno E *et al.* Reproductive biology characteristics of red mullet (*Mullus barbatus* L., 1758) in Southern Adriatic Sea and management implications. *Aquat Living Resour* 2015;**28**:21–31. https://doi.org/10.1051/alr/2015005

Carbonara P, Zupa W, Anastasopoulou A *et al.* Explorative analysis on red mullet (*Mullus barbatus*) ageing data variability in the Mediterranean. *Sci Mar* 2019;**83**:271–9. https://doi.org/10.3989/scimar

Charnov EL. Fish growth: bertalanffy k is proportional to reproductive effort. *Environ Biol Fish* 2008;**83**:185–7. https://doi.org/10.1007/s10641-007-9315-5

Chérif M, Ben Amor M, Selmi S *et al.* Food and feeding habits of the red mullet, *Mullus barbatus* (Actinopterygii: perciformes: mullidae), off the northern Tunisian coast (central Mediterranean). *Acta Ichth Pisc* 2011;**41**:109–16. https://doi.org/10.3750/AIP2011.41.2.06

Chimienti G, De Padova D, Adamo M *et al.* Effects of global warming on Mediterranean coral forests. *Sci Rep* 2021;**11**:20703. https://doi.org/10.1038/s41598-021-00162-4

Chung MT, Trueman CN, Godiksen JA *et al.* Field metabolic rates of teleost fishes are recorded in otolith carbonate. *Commun Biol* 2019;**2**:24. https://doi.org/10.1038/s42003-018-0266-5

Ciannelli L, Chan KS, Bailey KM, Stenseth NC, Nonadditive effects of the environment on the survival of a large marine fish population. *Ecology* 2004;**85**:3418–3427. https://doi.org/10.1890/03-0755

Cibic T, Baldassarre L, Cerino F *et al.* Benthic and Pelagic Contributions to Primary Production: Experimental Insights From the Gulf of Trieste (Northern Adriatic Sea). *Front Mar Sci* 2022;**9**:877935. https://doi.org/10.3389/fmars.2022.877935

Coggins LG, Gwinn DC, Allen MS. Evaluation of age length key sample sizes required to estimate fish total mortality and growth. *Trans Am Fish Soc* 2013;**142**:832–40. https://doi.org/10.1080/00028487.2013.768550

Copernicus Climate Change Service. *Climate Data Store: marine biogeochemistry data for the Northwest European Shelf and Mediterranean Sea from 2006 up to 2100 derived from climate projections*. Copernicus Climate Change Service (C3S) Climate Data Store (CDS). 2020. https://doi.org/10.24381/cds.dcc9295c.

Dalgleish HJ, Koons DN, Adler PB. Can life-history traits predict the response of populations to changes in climate variability? *J Ecol* 2010;**98**:209–17. https://doi.org/10.1111/j.1365-2745.2009.01585.x

Daufresne M, Lengfellner K, Sommer U. Global warming benefits the small in aquatic ecosystems. *Proc Natl Acad Sci USA* 2009;**106**:12788–93. https://doi.org/10.1073/pnas.0902080106

Debes PV, Fraser DJ, Yates M *et al.* The between-population genetic architecture of growth, maturation, and plasticity in Atlantic salmon. *Genetics* 2014;**196**:1277–91. https://doi.org/10.1534/genetics.114.161729

Edeline E. Adaptive phenotypic plasticity of eel diadromy. *Mar Ecol Prog Ser* 2007;**341**:229–32. https://doi.org/10.3354/meps341229

Enberg K, Jørgensen C, Dunlop ES *et al.* Fishing-induced evolution of growth: concepts, mechanisms and the empirical evidence. *Mar Ecol* 2012;**33**:1–25. https://doi.org/10.1111/j.1439-0485.2011.00460.x

Engen S, Cao FJ, Sæther BE, The effect of harvesting on the spatial synchrony of population fluctuations. *Theor Popul Biol* 2018;**123**:28–34. https://doi.org/10.1016/j.tpb.2018.05.001

Essington ET, Beaudreau AH, Wiedenmann J. Fishing through marine food webs. *Proc Natl Acad Sci USA* 2006;**103**:3171–5. https://doi.org/10.1073/pnas.0510964103

Fatima N, Shuaib SE, Kong JD. Predicting adaptations of fish and fishing communities to rapid climate velocities in Canadian waters: a systematic review. *Environ Adv* 2023;**14**:100452. https://doi.org/10.1016/j.envadv.2023.100452

Fiorentino F, Badalamenti F, D'Anna G *et al.* Changes in spawning-stock structure and recruitment pattern of red mullet, *Mullus barbatus*, after a trawl ban in the Gulf of Castellammare (central Mediterranean Sea). *ICES J Mar Sci* 2008;**65**:1175–83. https://doi.org/10.1093/icesjms/fsn104

Gokul T, Kumar KR, Prema P *et al.* Particulate pollution and its toxicity to fish: an overview. *Comp Biochem Physiol C Comp Pharmacol Toxicol* 2023;**270**:109646. https://doi.org/10.1016/j.cbpc.2023.109646

Grønkjær P. Otoliths as individual indicators: a reappraisal of the link between fish physiology and otolith characteristics. *Mar Freshw Res* 2016;**67**:881–8. https://doi.org/10.1071/MF15155

Heino M, Godø OR. Fisheries-induced selection pressures in the context of sustainable fisheries. *Bull Mar Sci* 2002;**70**:639–56.

Heino M, Kaitala V, Ranta E, Lindström J, Synchronous dynamics and rates of extinction in spatially structured populations. *Proc R Soc Lond B Biol Sci* 1997;**264**:481–486. https://doi.org/10.1098/rspb.1997.0069

Heino M, Kaitala V. Optimal resource allocation between growth and reproduction in clams: why does indeterminate growth exist? *Funct Ecol* 1996;**10**:245–51. https://doi.org/10.2307/2389849

Hobday AJ, Smith ADM, Stobutzki IC *et al.* Ecological risk assessment for the effects of fishing. *Fish Res* 2011;**108**:372–84. https://doi.org/10.1016/j.fishres.2011.01.013

Hollins J, Thambithurai D, Koeck B *et al.* A physiological perspective on fisheries-induced evolution. *Evol Appl* 2018;**11**:561–76. https://doi.org/10.1111/eva.12597

Hüssy K, Radtke K, Plikshs M *et al.* Challenging ICES age estimation protocols: lessons learned from the eastern Baltic cod stock. *ICES J Mar Sci* 2016;**73**:2138–49. https://doi.org/10.1093/icesjms/fsw107.

ICES. *Report of the Workshop on Age Reading of Red mullet Mullus barbatus and Striped mullet Mullus surmuletus (WKACM)*, 30 March–3 April 2009, Boulogne sur Mer, France. ICES CM 2009/ACOM: 44`, 42 pp. Available at: https://www.ices.dk/sites/pub/CM%20Doccuments/CM-2009/ACOM/ACOM4409.pdf#search=age%20mullus

Jennings S, Pinnegar J, Polunin N *et al.* Impacts of trawling disturbance on the trophic structure of benthic invertebrate communities. *Mar Ecol Prog Ser* 2001;**213**:127–42. http://www.jstor.org/stable/24864207

Karametsidis G, Rueda L, Bellido JM *et al.* The trade-off between condition and growth shapes juveniles' survival of harvested demersal fish of the Mediterranean Sea. *Mar Environ Res* 2023;**184**:105844. https://doi.org/10.1016/j.marenvres.2022.105844

Kimura DK, Lyons JJ. Between-reader bias and variability in the age-determination process. *Fish Bull* 1991;**89**:53–60.

Kjesbu OS, Bogstad B, Devine JA *et al.* Synergies between climate and management for Atlantic cod fisheries at high latitudes. *Proc Natl Acad Sci USA* 2014;**111**:3478–3483. https://doi.org/10.1073/pnas.1316342111

Kraak SBM, Haase S, Minto C *et al.* The Rosa Lee phenomenon and its consequences for fisheries advice on changes in fishing mortality or gear selectivity. *ICES J Mar Sci* 2019;**76**:2179–92. https://doi.org/10.1093/icesjms/fsz107

Kuehn B. *Tutorial—ways to bias correct climate projections*. Figshare. 2023. https://doi.org/10.6084/m9.figshare.23514618.v1

Le Bris A, Mills KE, Wahle RA *et al.* Climate vulnerability and resilience in the most valuable North American fishery. *Proc Natl Acad Sci USA* 2018;**115**:1831–1836. https://doi.org/10.1073/pnas.1711122115

Lee Q, Punt AE. Extracting a time-varying climate-driven growth index from otoliths for use in stock assessment models. *Fish Res* 2018;**200**:93–103. https://doi.org/10.1016/j.fishres.2017.12.014

Lembo G, Spedicato MT. Caratterizzazione ambientale delle aree di pesca: GSA 18–adriatico Meridionale. Roma. In: Cataudella S, Spagnolo (eds.) *Lo stato della pesca e dell'acquacoltura nei mari Italiani*, Monografie Scientifiche Ministero delle Politiche Agricole, Alimentari e Forestali (Italy). 2011, pp.79–87. https://www.politicheagricole.it/flex/cm/pages/ServeBLOB.php/L/IT/IDPagina/6412

Lester NP, Shuter BJ, Abrams PA. Interpreting the von Bertalanffy model of somatic growth in fishes: the cost of reproduction. *Proc Biol Sci* 2004;**271**:1625–31. https://doi.org/10.1098/rspb.2004.2778

Lobón-Cerviá J., Why, when and how do fish populations decline, collapse and recover? The example of brown trout (Salmo trutta) in Rio Chaballos (northwestern Spain). *Freshw Biol* 2009;**54**:1149–1162. https://doi.org/10.1111/j.1365-2427.2008.02159.x

Lojo D, Cousido-Rocha M, Cerviño S *et al.* Assessing changes in size at maturity for the European hake (*Merluccius merluccius*) in Atlantic Iberian waters. *Sci Mar* 2022;**86**:e046. https://doi.org/10.3989/scimar

Lombarte A, Aguirre H. Quantitative differences in the chemoreceptor systems in the barbels of two species of Mullidae (*Mullus surmuletus* and *M. barbatus*) with different bottom habitats. *Mar Ecol Prog Ser* 1997;**150**:57–64. https://doi.org/10.3354/meps150057

López-Abellán LJ, Santamaría MTG, González JF. Approach to ageing and growth back-calculation based on the otolith of the southern boarfish *Pseudopentaceros richardsoni* (Smith, 1844) from the south-west Indian Ocean sea mounts. *Mar Freshw Res* 2008;**59**:269–78. https://doi.org/10.1071/MF07131

Mangano MC, Bottari T, Porporato EMD *et al.* The effectiveness of fish feeding behaviour in mirroring trawling-induced patterns. *Mar Environ Res* 2017;**131**:195–204. https://doi.org/10.1016/j.marenvres.2017.09.004

Maravelias CD, Tsitsika EV, Papaconstantinou C. Environmental influences on the spatial distribution of european hake (*Merluccius merluccius*) and red mullet (*Mullus barbatus*) in the Mediterranean. *Ecol Res* 2007;**22**:678–85. https://doi.org/10.1007/s11284-006-0309-0

Marra G, Wood SN. Practical variable selection for generalized additive models. *Comput Stat Data Anal* 2011;**55**:2372–87. https://doi.org/10.1016/j.csda.2011.02.004

Martino JC, Fowler AJ, Doubleday ZA *et al.* Using otolith chronologies to understand long-term trends and extrinsic drivers of growth in fisheries. *Ecosphere* 2019;**10**:e02553. https://doi.org/10.1002/ecs2.2553

Massa P, Leitão H, Manousaki T *et al.* Genomic insights into the population structure and adaptive variation of *Mullus barbatus* in the Mediterranean Sea. *BMC Ecol Evo* 2025;**25**:101. https://doi.org/10.1186/s12862-025-02443-2

Matic-Skoko S, Šegvic-Bubic T, Mandic I *et al.* Evidence of subtle genetic structure in the sympatric species *Mullus barbatus* and *Mullus surmuletus* (Linnaeus, 1758) in the Mediterranean Sea. *Sci Rep* 2018;**8**:1–14. https://doi.org/10.1038/s41598-017-18503-7

Matthias BG, Ahrens RMN, Allen MS *et al.* Understanding the effects of density and environmental variability on the process of fish growth. *Fish Res* 2018;**198**:209–19. https://doi.org/10.1016/j.fishres.2017.08.018

Morrongiello JR, Horn PL, Maolagáin CÓ *et al.* Synergistic effects of harvest and climate drive synchronous somatic growth within key New Zealand fisheries. *Glob Change Biol* 2025;**27**:1470–84. https://doi.org/10.1111/gcb.15490

Morrongiello JR, Sweetman PC, Thresher RE . Fishing constrains phenotypic responses of marine fish to climate variability. *J Anim Ecol* 2019;**88**:1645–56. https://doi.org/10.1111/1365-2656.12999

Morrongiello JR, Thresher RE. A statistical framework to explore ontogenetic growth variation among individuals and populations: a marine fish example. *Ecol Monogr* 2015;**85**:93–115. https://doi.org/10.1890/13-2355.1

Neuheimer AB, Thresher RE, Lyle JM *et al.* Tolerance limit for fish growth exceeded by warming waters. *Nat Clim Chan* 2011;**1**:110–3. https://doi.org/10.1038/nclimate1084

Ng CZ, Gonzalez JG, Saleh MF *et al.* Contrasting environmental and demographic influences on growth variability in two tropical snappers spanning the equator in the Indo-West Pacific. *Rev Fish Biol Fish* 2025;**35**:565–85. https://doi.org/10.1007/s11160-025-09923-0

Öckinger E, Schweiger O, Crist TO *et al.* Life-history traits predict species responses to habitat area and isolation: a cross-continental synthesis. *Ecol Lett* 2010;**13**:969–79. https://doi.org/10.1111/j.1461-0248.2010.01487.x

Paradinas I, Conesa D, López-Quílez A *et al.* Assessing the spatiotemporal persistence of fish distributions: a case study on two red mullet species (*Mullus surmuletus* and *M. barbatus*) in the western Mediterranean. *Mar Ecol Prog Ser* 2020;**644**:173–85. https://doi.org/10.3354/meps13366

Pepin P. Reconsidering the impossible—linking environmental drivers to growth, mortality, and recruitment of fish. *Can J Fish*

Aquat Sci 2015;**73**:205–15. https://doi.org/10.1139/cjfas-2015-0091

Pilling GM, Kirkwood GP, Walker SG. An improved method for estimating individual growth variability in fish, and the correlation between von Bertalanffy growth parameters. *Can J Fish Aquat Sci* 2002;**59**:424–32. https://doi.org/10.1139/f02-022

Planque B, Fromentin JM, Cury P *et al.* How does fishing alter marine populations and ecosystems sensitivity to climate? *J Mar Syst* 2010;**79**:403–17. https://doi.org/10.1016/j.jmarsys.2008.12.018

R Core Team. R: a language and environment for statistical computing. https://www.R-project.org. 2026.

Ragnarsson S, Lindegarth M. Testing hypotheses about temporary and persistent effects of otter trawling on infauna: changes in diversity rather than abundance. *Mar Ecol Prog Ser* 2009;**385**:51–64. https://doi.org/10.3354/meps08056

Rahikainen M, Stephenson RL. Consequences of growth variation in northern Baltic herring for assessment and management. *ICES J Mar Sci* 2004;**61**:338–50. https://doi.org/10.1016/j.icesjms.2004.02.005

Reale M, Cossarini G, Lazzari P *et al.* Acidification, deoxygenation, and nutrient and biomass declines in a warming Mediterranean Sea. *Biogeosciences* 2022;**19**:4035–65. https://doi.org/10.5194/bg-19-4035-2022:

Reeves SA. A simulation study of the implications of agereading errors for stock assessment and management advice. *ICES J Mar Sci* 2003;**60**:314–28. https://doi.org/10.1016/S1054-3139(03)00011-0

Riahi K, Rao S, Krey V *et al.* RCP 8.5—A scenario of comparatively high greenhouse gas emissions. *Clim Change* 2011;**109**:33–57. https://doi.org/10.1007/s10584-011-0149-y

Ricci F, Capellacci S, Casabianca S *et al.* Variability of hydrographic and biogeochemical properties in the North-western Adriatic coastal waters in relation to river discharge and climate changes. *Chemosphere* 2024;**301**:142486. https://doi.org/10.1016/j.chemosphere.2024.142486

Rogers LA, Dougherty AB, Effects of climate and demography on reproductive phenology of a harvested marine fish population. *Glob Change Biol* 2018;**25**:708–720. https://doi.org/10.1111/gcb.14483

Rossi V, Sammartino I, Pellegrini C *et al.* Coupling palaeobiology and geochemistry from the Holocene of the southern Adriatic Sea (Gulf of Manfredonia, Italy): shelf facies patterns and eutrophication trends. *Palaeogeogr Palaeoclimatol Palaeoecol* 2024;**634**:112055. https://doi.org/10.1016/j.palaeo.2024.112055

Rouyer T, Sadykov A, Ohlberger J, Stenseth NC, Does increasing mortality change the response of fish populations to environmental fluctuations?. *Ecol Lett* 2012;**15**:658–665. https://doi.org/10.1111/j.1461-0248.2012.01781.x

Schindler DE, Hilborn R, Chasco B *et al.* Population diversity and the portfolio effect in an exploited species. *Nature* 2010;**465**:609–612. https://doi.org/10.1038/nature09060

Silva A, Carrera P, MassP J *et al.* Geographic variability of sardine growth across the northeastern Atlantic and the Mediterranean Sea. *Fish Res* 2008;**90**:56–69. https://doi.org/10.1016/j.fishres.2007.09.011

Sinopoli M, Andaloro F, Agnetta D *et al.* Bottom trawling affects trophic niche diversity of red mullet in muddy bottoms of the Mediterranean continental shelf. *Mar Environ Res* 2025;**211**:107398. https://doi.org/10.1016/j.marenvres.2025.107398

Smith BJ, Dembkowski DJ, James DA *et al.* A Simple Method to Reduce Interpretation Error of Ages Estimated from Otoliths. *Open Fish Sci J* 2016;**9**:1–7. https://doi.org/10.2174/1874401×01609010001

Sogard SM. Size-selective mortality in the juvenile stage of teleost fishes: a review. *Bull Mar Sci* 1997;**60**:1129–57

Spedicato MT, Massutí E, Mérigot B *et al.* The MEDITS trawl survey specifications in an ecosystem approach to fishery management. *Sci Mar* 2019;**83**:9–20. https://doi.org/10.3989/scimar.04915.11X

Stawitz CC, Essington TE. Somatic growth contributes to population variation in marine fishes. *J Anim Ecol* 2019;**88**:315–29. https://doi.org/10.1111/1365-2656.12921

Stawitz CC, Essington TE, Branch TA *et al.* A state-space approach for detecting growth variation and application to North Pacific groundfish. *Can J Fish Aquat Sci* 2015;**72**:1316–28. https://doi.org/10.1139/cjfas-2014-0558

Strom A, Francis RC, Mantua NJ *et al.* North Pacific climate recorded in growth rings of geoduck clams: a new tool for paleoenvironmental reconstruction. *Geophys Res Lett* 2004;**31**:L06206. https://doi.org/10.1029/2004GL019440

Taslima K, Al-Emran M, Rahman MS *et al.* Impacts of heavy metals on early development, growth and reproduction of fish—A review. *Tox Rep* 2022;**9**:858–68. https://doi.org/10.1016/j.toxrep.2022.04.013

Thorson JT, Minte-Vera CV. Relative magnitude of cohort, age, and year effects on size at age of exploited marine fishes. *Fish Res* 2016;**180**:45–53. https://doi.org/10.1016/j.fishres.2014.11.016

Tserpes G, Fiorentino F, Levi D *et al.* Distribution of *Mullus barbatus* and *M. surmuletus* (Osteichthyes: perciformes) in the Mediterranean continental shelf: implications for management. *Sci Mar* 2002;**66**:39–54. https://doi.org/10.3989/scimar.2002.66s239

Tserpes G, Massutí E, Fiorentino F *et al.* Distribution and spatio-temporal biomass trends of red mullets across the Mediterranean. *Sci Mar* 2019;**83**:43–55. https://doi.org/10.3989/scimar.04888.21A

Tursi A, D'Onghia G, Sion L *et al.* Caratterizzazione ambientale delle aree di pesca: gSA19–mar Ionio occidentale. In: Cataudella S, Spagnolo (eds.), *Lo stato della pesca e dell'acquacoltura nei mari Italiani*, Monografie Scientifiche Ministero delle Politiche Agricole, Alimentari e Forestali (Italy), 2011;88–94. Available at: https://www.politicheagricole.it/flex/cm/pa ges/ServeBLOB.php/L/IT/IDPagina/6412

Uusi-Heikkilä S, Whiteley AR, Kuparinen A *et al.* The evolutionary legacy of size-selective harvesting extends from genes to populations. *Evol Appl* 2015;**8**:597–620. https://doi.org/10.1111/eva.12268

Vassilopoulou V, Papaconstantinou C. Feeding habits of red mullet (*Mullus barbatus*) in a gulf in western Greece. *Fish Res* 1993;**16**:69–83. https://doi.org/10.1016/0165-7836(93)90110-S

Vilibic I, Orlic M. Adriatic water masses, their rates of formation and transport through the Otranto Strait. *Deep Sea Res I Oceanogr Res Pap* 2002;**49**:1321–40. https://doi.org/10.1016/S0967-0637(02)00028-6

Wakefield CB, Potter IC, Hall NG *et al.* Timing of growth zone formations in otoliths of the snapper, *Chrysophrys auratus*, in subtropical and temperate waters differ and growth follows a parabolic relationship with latitude. *ICES J Mar Sci* 2016;**74**:180–92. https://doi.org/10.1093/icesjms/fsw137

Wang YG, Ellis N. Effect of individual variability on estimation of population parameters from length-frequency data. *Can J Fish Aquat Sci* 1998;**55**:2393–401. https://doi.org/10.1139/cjfas-55-11-2393

Weisberg S. Using hard-part increment data to estimate age and environmental effects. *Can J Fish Aquat Sci* 1993;**50**:1229–37. https://doi.org/10.1139/f93-139

Widdrington JB, Reis-Santos P, Morrongiello JR *et al.* Otolith growth chronologies reveal distinct environmental sensitivities between and within shallow-and deep-water snappers. *Rev Fish Biol Fish* 2025;**35**:217–40. https://doi.org/10.1007/s11160-024-09898-4

Wood SN. *Generalized Additive Models. An Introduction with R*. 2nd ed. Chapman and Hall/CRC, 2017, 496. https://doi.org/10.1201/9781315370279

Zupa W, Carbonara P, Bitetto I *et al.* Relative benthic status guides sustainable trawl management in the Adriatic–Ionian Seas. *ICES J Mar Sci* 2025;**82**:fsaf148. https://doi.org/10.1093/icesjms/fsaf148

Handling Editor: Francis Juanes

Received: 23 December 2025. **Revised:** 30 June 2026. **Accepted:** 1 July 2026